

## Physical, Thermal and Spectroscopic Characterization of m-Toluic Acid: an Impact of Biofield Treatment

Mahendra Kumar Trivedi<sup>1</sup>, Alice Branton<sup>1</sup>, Dahryni Trivedi<sup>1</sup>, Gopal Nayak<sup>1</sup>, Ragini Singh<sup>2</sup> and Snehasis Jana<sup>2\*</sup>

<sup>1</sup>Trivedi Global Inc., 10624 S Eastern Avenue Suite A-969, Henderson, NV 89052, USA

<sup>2</sup>Trivedi Science Research Laboratory Pvt. Ltd., Hall-A, Chinar Mega Mall, Chinar Fortune City, Hoshangabad Rd, Bhopal- 462026, Madhya Pradesh, India

### Abstract

m-toluic acid (MTA) is widely used in manufacturing of dyes, pharmaceuticals, polymer stabilizers, and insect repellents. The aim of present study was to evaluate the impact of biofield treatment on physical, thermal and spectroscopic properties of MTA. MTA sample was divided into two groups that served as treated and control. The treated group received Mr. Trivedi's biofield treatment. Subsequently, the control and treated samples were evaluated using X-ray diffraction (XRD), surface area analyser, differential scanning calorimetry (DSC), thermogravimetric analysis (TGA), Fourier transform infrared (FT-IR) and ultraviolet-visible (UV-Vis) spectroscopy. XRD result showed a decrease in crystallite size in treated samples *i.e.* 42.86% in MTA along with the increase in peak intensity as compared to control. However, surface area analysis showed an increase in surface area of 107.14% in treated MTA sample as compared to control. Furthermore, DSC analysis results showed that the latent heat of fusion was considerably reduced by 40.32%, whereas, the melting temperature was increased (2.23%) in treated MTA sample as compared to control. The melting point of treated MTA was found to be 116.04°C as compared to control (113.51°C) sample. Moreover, TGA/DTG studies showed that the control sample lost 56.25% of its weight, whereas, in treated MTA, it was found 58.60%. Also,  $T_{max}$  (temperature, at which sample lost maximum of its weight) was decreased by 1.97% in treated MTA sample as compared to control. It indicates that the vapourisation temperature of treated MTA sample might decrease as compared to control. The FT-IR and UV-Vis spectra did not show any significant change in spectral properties of treated MTA sample as compared to control. These findings suggest that biofield treatment has significantly altered the physical and thermal properties of m-toluic acid, which could make them more useful as a chemical intermediate.

**Keywords:** Biofield treatment; m-Toluic acid; X-ray diffraction study; Surface area analysis; Differential scanning calorimetry; Thermogravimetric analysis; Fourier transform infrared spectroscopy; Ultraviolet-visible spectroscopy

### Introduction

The m-toluic acid (MTA) is a benzoic acid derivative having a floral honey odour. Benzoic acid occurs naturally in many plants and its name was also derived from a plant source *i.e.* Gum benzoin. Although it is used as precursor to plasticizers, preservatives such as sodium benzoate, it also has wide application in many pharmaceutical preparations meant for treatment of fungal skin diseases, topical antiseptics, expectorants, analgesics and decongestants [1,2]. The benzoic acid derivatives are also very useful due to their bacteriostatic and fragrant properties. They are used as intermediate in the production of various pharmaceuticals having analgesic, antirheumatic and vasodilator properties [3]. MTA is used as a chemical intermediate in manufacturing of insect repellent and plastic stabilizer in the chemical industry. It is also used in the production of various chemicals like 3-carboxybenzaldehyde, 3-benzoylphenylacetic acid, 3-methylbenzophenone, and N,N-diethyl-3-methylbenzamide *etc.* [4,5]. It is a main component of N,N-diethyl-m-toluamide, commonly known as DEET, which is first insect repellent that can be applied to skin or clothing and provide protection against mosquitoes and other biting insects [6].

MTA is used as intermediate in various chemical reactions, hence its rate of reaction plays a crucial role. It was reported previously that any alteration in crystallite size and surface area can affect the kinetics of reaction [7]. Moreover, the rate kinetics of any chemical reaction also depends on the thermal properties of the intermediate chemical compound *i.e.* latent heat of fusion, vapourisation temperature, decomposition temperature *etc.* [8]. After considering the properties and applications of MTA, authors wanted to investigate an economically safe approach that could be beneficial to modify their physical, thermal and spectral properties.

The concept of human bioenergy has its origin thousands of years back. It is scientifically termed as the biologically produced electromagnetic and subtle energy field that provides regulatory and communication functions within the human organs [9]. It generates through internal physiological processes such as blood flow, brain and heart function, *etc.* Nowadays, many biofield therapies are in practice for their possible therapeutic potentials such as enhanced personal well-being, improved functional ability of arthritis patient, decreased pain and anxiety [10-12]. The practitioners of these therapy claim that the healers channel supraphysical energy and intentionally direct this energy towards target [13]. Thus, a human has the ability to harness the energy from environment or universe and can transmit into any living or non-living object(s). The objects always receive the energy and responding into useful way that is called biofield energy and the process is known as biofield treatment.

Mr. Trivedi's biofield treatment (The Trivedi effect<sup>®</sup>) is well known and significantly studied in different fields such as microbiology [14-16], agriculture [17,18], and biotechnology [19]. Exposure to biofield energy caused an increase in medicinal property, growth, and

**\*Corresponding author:** Snehasis Jana, Trivedi Science Research Laboratory Pvt. Ltd., Hall-A, Chinar Mega Mall, Chinar Fortune City, Hoshangabad Rd, Bhopal- 462026, Madhya Pradesh, India, Tel: +91-755-666-0006; E-mail: [publication@trivedisrl.com](mailto:publication@trivedisrl.com)

Received July 25, 2015; Accepted August 03, 2015; Published August 06, 2015

**Citation:** Trivedi MK, Branton A, Trivedi D, Nayak G, Singh R, et al. (2015) Physical, Thermal and Spectroscopic Characterization of m-Toluic Acid: an Impact of Biofield Treatment. Biochem Pharmacol (Los Angel) 4: 178. doi:10.4172/2167-0501.1000178

**Copyright:** © 2015 Trivedi MK, et al. This is an open-access article distributed under the terms of the Creative Commons Attribution License, which permits unrestricted use, distribution, and reproduction in any medium, provided the original author and source are credited.

anatomical characteristics of ashwagandha [20]. Recently, the impact of biofield treatment on atomic, crystalline and powder characteristics as well as spectroscopic characters of different materials was studied [21,22]. The biofield treatment had increased the particle size by six fold and enhanced the crystallite size by two fold in zinc powder [23]. Hence, based on the outstanding results obtained after biofield treatment on different materials and considering the pharmaceutical applications of MTA, the present study was undertaken to evaluate the impact of biofield treatment on physical, thermal and spectroscopic properties of MTA.

## Materials and Methods

m-toluic acid (MTA) was procured from S D Fine Chemicals Pvt. Ltd., India. The sample was divided into two parts; one was kept as a control, while other was subjected to Mr. Trivedi's biofield treatment and coded as treated sample. The treatment sample in sealed pack was handed over to Mr. Trivedi for biofield treatment under standard laboratory conditions. Mr. Trivedi provided the treatment through his energy transmission process to the treated group without touching the sample. The biofield treated sample was returned in the similarly sealed condition for further characterization using XRD, surface area analyser, DSC, TGA, FT-IR and UV-Vis spectroscopic techniques.

### X-ray diffraction (XRD) study

XRD analysis was carried out on Phillips, Holland PW 1710 X-ray diffractometer system, which had a copper anode with nickel filter. The radiation of wavelength used by the XRD system was 1.54056 Å. The data obtained were in the form of a chart of  $2\theta$  vs. intensity and a detailed table containing peak intensity counts, d value (Å), peak width ( $\theta^\circ$ ), relative intensity (%) etc.

The crystallite size (G) was calculated by using formula:

$$G = k\lambda / (b \cos \theta)$$

Here,  $\lambda$  is the wavelength of radiation used; b is full width half maximum (FWHM) of peaks and k is the equipment constant (=0.94). However, percent change in crystallite size was calculated using the following equation:

$$\text{Percent change in crystallite size} = [(G_t - G_c) / G_c] \times 100$$

Where,  $G_c$  and  $G_t$  are crystallite size of control and treated powder samples respectively.

### Surface area analysis

The surface area was measured by the Surface area analyser, Smart SORB 90 based on Brunauer-Emmett-Teller (BET). Percent changes in surface area were calculated using following equation:

$$\text{\% change in surface area} = \frac{[S_{\text{Treated}} - S_{\text{Control}}]}{S_{\text{Control}}} \times 100$$

Where,  $S_{\text{Control}}$  and  $S_{\text{Treated}}$  are the surface area of control and treated samples respectively.

### Differential scanning calorimetry (DSC) study

For studies related to melting temperature and latent heat of fusion of MTA, Differential Scanning Calorimeter (DSC) of Perkin Elmer/Pyris-1, USA with a heating rate of 10°C/min under air atmosphere and flow rate of 5 ml/min was used. Melting temperature and latent heat of fusion were obtained from the DSC curve.

Percent change in latent heat of fusion was calculated using

following equations:

$$\text{\% change in Latent heat of fusion} = \frac{[\Delta H_{\text{Treated}} - \Delta H_{\text{Control}}]}{\Delta H_{\text{Control}}} \times 100$$

Where,  $\Delta H_{\text{Control}}$  and  $\Delta H_{\text{Treated}}$  are the latent heat of fusion of control and treated samples, respectively. Similarly, percent change in melting point was also calculated to observe the difference in thermal properties of treated MTA sample as compared to control.

### Thermogravimetric analysis/ Derivative Thermogravimetry (TGA/DTG)

Thermal stability of control and treated sample of MTA was analysed by using Mettler Toledo simultaneous Thermogravimetric analyser (TGA/DTG). The samples were heated from room temperature to 400°C with a heating rate of 5°C/min under air atmosphere. From TGA curve, onset temperature  $T_{\text{onset}}$  (temperature at which sample start losing weight) and from DTG curve,  $T_{\text{max}}$  (temperature at which sample lost its maximum weight) were recorded.

Percent change in temperature at which maximum weight loss occur in sample was calculated using following equation:

$$\text{\% change in } T_{\text{max}} = [(T_{\text{max, treated}} - T_{\text{max, control}}) / T_{\text{max, control}}] \times 100$$

Where,  $T_{\text{max, control}}$  and  $T_{\text{max, treated}}$  are the temperature at which maximum weight loss occurs in control and treated sample, respectively.

Percent change in onset peak temperature was calculated using following equation:

$$\text{\% change in onset peak temperature } T_{\text{onset}} = [(T_{\text{onset, treated}} - T_{\text{onset, control}}) / T_{\text{onset, control}}] \times 100$$

Where,  $T_{\text{onset, control}}$  and  $T_{\text{onset, treated}}$  are onset peak temperature in control and treated sample, respectively.

### Spectroscopic studies

For determination of spectroscopic characters, the treated sample was divided into two groups i.e. T1 and T2. Both treated groups were analysed for their spectral characteristics using FT-IR and UV-Vis spectroscopy as compared to control MTA sample.

### FT-IR spectroscopic characterization

FT-IR spectra were recorded on Shimadzu's Fourier transform infrared spectrometer (Japan) with the frequency range of 4000-500  $\text{cm}^{-1}$ . The samples are prepared by grinding the dry blended powders of control and treated MTA with powdered KBr, and then compressed to form discs. The FT-IR spectroscopic analysis of MTA (control, T1 and T2) were carried out to evaluate the impact of biofield treatment at atomic and molecular level like bond strength, stability, rigidity of structure etc. [24].

### UV-Vis spectroscopic analysis

The UV-Vis spectral analysis was measured using Shimadzu UV-2400 PC series spectrophotometer over a wavelength range of 200-400 nm with 1 cm quartz cell and a slit width of 2.0 nm. This analysis was performed to evaluate the effect of biofield treatment on the structural property of MTA sample. The UV-Vis spectroscopy gives the preliminary information related to the skeleton of chemical structure and possible arrangement of functional groups. With UV-Vis spectroscopy, it is possible to investigate electron transfers between orbitals or bands of atoms, ions and molecules existing in the gaseous,

liquid and solid phase [24].

## Results and Discussion

### X-ray diffraction

X-ray diffraction study was conducted to study the crystalline nature of the control and treated sample of MTA. XRD diffractograms of control and treated samples of MTA are shown in Figure 1. The XRD diffractogram of control MTA showed an intense crystalline peak at  $2\theta$  equals to  $14.00^\circ$ . The single intense peak indicated the crystalline nature of MTA. However, the XRD diffractogram of treated MTA showed the crystalline peak at  $2\theta$  equals to  $13.90^\circ$ . The treated sample peak showed high intensity as compared to control that indicated that crystallinity of treated MTA sample increased as compared to control. It is presumed that biofield energy may be absorbed by the treated MTA molecules that may lead to formation of more symmetrical crystalline long range pattern that caused increase in intensity of peak. In addition, the crystallite size was found to be 104.211 and 59.543 nm in control and treated MTA, respectively. The crystallite size was decreased by 42.86% in treated MTA as compared to control (Figure 2). The decreased crystallite size may be due to biofield energy that can induce strain in lattice and that possibly resulted in fracturing of grains into sub grains and hence decreased crystallite size [23]. MTA is used as intermediate in synthesis of many pharmaceutical compounds hence, decrease in

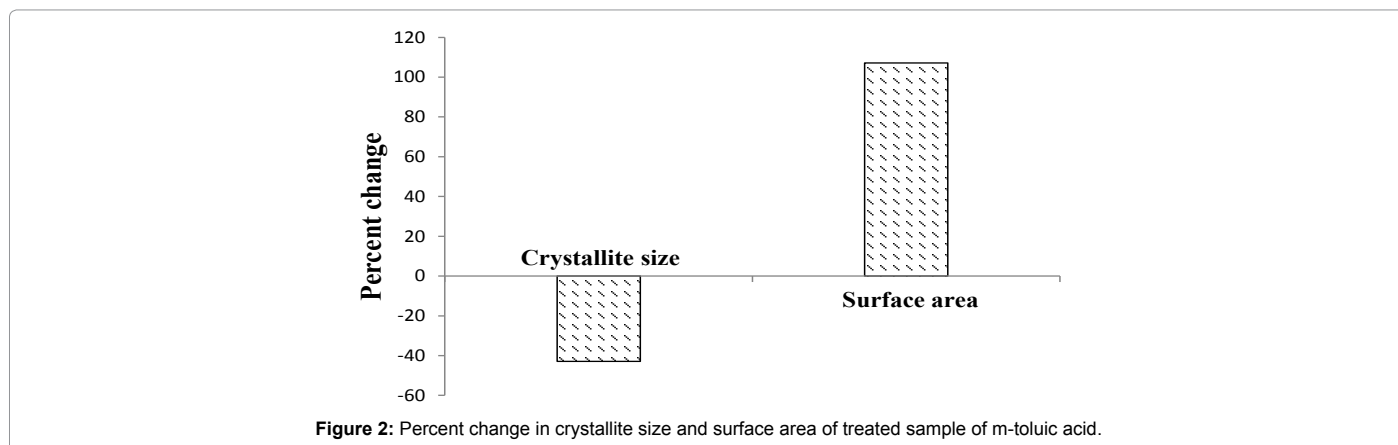
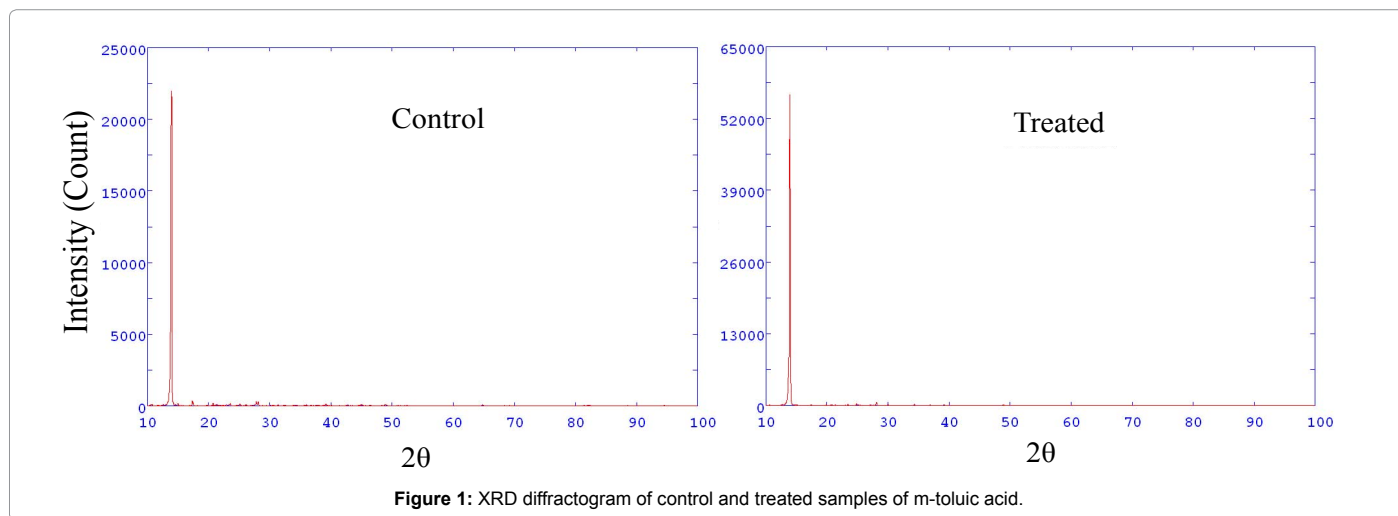
crystallite size may lead to fasten the rate kinetics which ultimately enhances the percentage yield of end products [8].

### Surface area analysis

The surface area of control and treated samples of MTA were investigated using BET method. The control sample showed a surface area of  $0.14 \text{ m}^2/\text{g}$  however, the treated sample of MTA showed a surface area of  $0.29 \text{ m}^2/\text{g}$ . The percentage increase in surface area was 107.14% in the treated MTA sample as compared to control (Figure 2). The XRD results of treated MTA sample revealed that crystallite size decreased after biofield treatment. It could be a possible reason for increase in surface area of treated MTA sample [25]. Moreover, increase in surface area of reactant molecules fastens the rate of reaction [26]. Hence, it is hypothesized that increase in surface area of treated MTA sample can be used to increase the rate of those reactions where MTA is used as intermediate reagent.

### Thermal studies

**DSC analysis:** DSC was used to determine  $\Delta H$  and melting temperature in control and treated sample of MTA. The DSC thermograms of control and treated samples of MTA are shown in Figure 3 and the analysis results are presented in Table 1. In a solid, the amount of energy required to change the phase from solid to liquid is known as latent heat of fusion ( $\Delta H$ ). Further, the energy supplied during phase change *i.e.*  $\Delta H$  is stored as potential energy of atoms. The



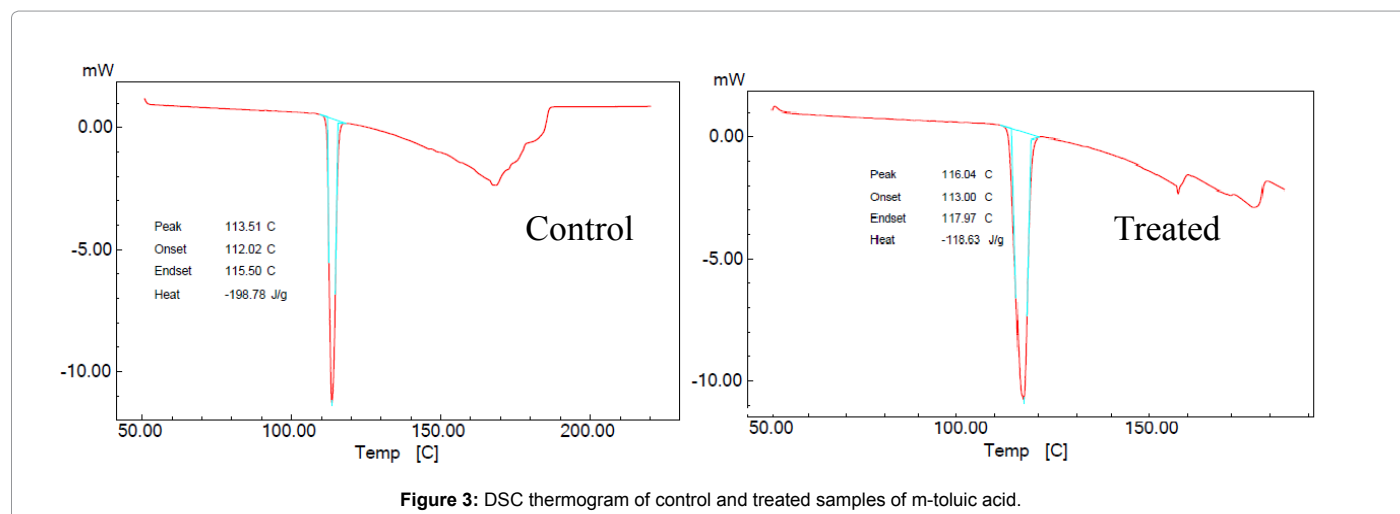


Figure 3: DSC thermogram of control and treated samples of m-toluic acid.

Parameter	Control	Treated
Latent heat of fusion $\Delta H$ (J/g)	198.78	118.63
Melting point ( $^{\circ}\text{C}$ )	113.51	116.04
$T_{\text{max}}$ ( $^{\circ}\text{C}$ )	187.02	183.32
Weight loss (%)	56.25	58.60

$T_{\text{max}}$ : temperature at which maximum weight loss occur

Table 1: Thermal analysis of control and treated sample of m-Toluic acid.

data showed that  $\Delta H$  was reduced from 198.78 J/g (control) to 118.63 J/g in treated MTA. It indicates that  $\Delta H$  was decreased by 40.32% in treated sample as compared to control (Figure 5). The reduction in  $\Delta H$  revealed that treated MTA probably have extra internal energy in the form of potential energy as compared to control, which might be transferred through biofield treatment. This potential energy may be stored in treated MTA molecules, that could lead to lowering of  $\Delta H$  in treated sample as compared to control. However, the melting temperature is related to the kinetic energy of the atoms [27]. The melting temperature of treated MTA was increased from 113.51 $^{\circ}\text{C}$  (control) to 116.04 $^{\circ}\text{C}$ . Thus, data suggest that melting point was increased by 2.23% as compared to control (Figure 5). Previously, our group reported that biofield treatment has altered  $\Delta H$  and melting point in lead and tin powder [28]. Besides, the increase of melting point in treated MTA suggests that kinetic energy and thermal vibrations of molecules probably altered after biofield treatment. In addition, the sharpness of the endothermic peaks showed a good degree of crystallinity in control and treated sample of MTA.

**TGA/DTG analysis:** Thermogravimetric analysis/derivative thermogravimetry analysis (TGA/DTG) of control and biofield treated samples are summarized in Table 1. TGA thermogram (Figure 4) showed that control MTA sample started losing weight around 170 $^{\circ}\text{C}$  (onset) and stopped near 212 $^{\circ}\text{C}$  (end set). However, the treated MTA started losing weight near to 164 $^{\circ}\text{C}$  (onset) and terminated near 209 $^{\circ}\text{C}$  (end set). It indicates that onset temperature of treated MTA decreased by 3.52% as compared to control (Figure 5). Furthermore, in this process, control sample lost 56.25% and treated MTA sample lost 58.60% of its weight, which could be due to vaporisation of MTA. Besides, DTG thermogram data showed  $T_{\text{max}}$  at 187.02 $^{\circ}\text{C}$  in control, whereas, it was decreased to 183.32 $^{\circ}\text{C}$  in treated MTA (Table 1). It indicates that  $T_{\text{max}}$  was decreased by 1.97% in treated MTA (Figure 5). Furthermore, the reduction in  $T_{\text{max}}$  in treated MTA with respect to control sample may be correlated with increase in vaporisation

of treated MTA after biofield treatment. A possible reason for this reduction in  $T_{\text{max}}$  is that biofield energy might cause some alteration in internal energy which results into earlier vaporisation of treated MTA sample as compared to control. Moreover, it was previously reported that the state of reactant affect rate of reaction, *i.e.* gases reacts faster than solid and liquids because gases consumed less energy to separate their particles from each other [26]. Also, decrease in vaporisation temperature indicates that MTA molecules change their phase from liquid to vapour at low temperature, which may result in more frequent collision of MTA molecules with other reactants at low temperature, hence fasten the reaction rate [26]. Apart from that, it was previously reported that vapour phase reaction can be more advantageous as compared to liquid phase reaction in terms of reaction time, generation of objectionable amounts of odour and undesired by-products [29,30]. Hence, overall observations suggest that biofield treated MTA can be used to enhance the reaction kinetics and yield of the end product.

### Spectroscopic studies

**FT-IR analysis:** FT-IR spectra of control, T1 and T2 samples of MTA are shown in Figure 6. It showed similar distribution patterns for both control and treated (T1 and T2) samples of MTA. The O-H stretching (carboxylic acid) peak was appeared at 3061-2576  $\text{cm}^{-1}$  in control MTA. In treated samples, O-H stretching (carboxylic acid) peak appeared in same range *i.e.* 3061-2576  $\text{cm}^{-1}$  in T1 and 3064-2576  $\text{cm}^{-1}$  in T2 sample. The peak due to C-H stretching ( $\text{sp}_3$ ) was appeared at 2951, 2953 and 2951  $\text{cm}^{-1}$  in control, T1 and T2 sample respectively. The C=O stretching (carboxylic acid) peak was appeared at 1689  $\text{cm}^{-1}$  in control and 1685  $\text{cm}^{-1}$  in both T1 and T2 samples. The peak due to aromatic C=C stretching was appeared at 1608  $\text{cm}^{-1}$  in all three samples *i.e.* control, T1 and T2. Similarly C-C stretching peak (in ring) was found at 1589  $\text{cm}^{-1}$  in all three samples *i.e.* control, T1 and T2. O-H bending peak was found at 1417, 1415 and 1417  $\text{cm}^{-1}$  in control, T1 and T2 sample respectively. C-O stretching (carboxylic acid) peak was appeared at 1311  $\text{cm}^{-1}$  in all three samples *i.e.* control, T1 and T2. Similarly, C-OH stretching peak appeared at 1217  $\text{cm}^{-1}$  in all three samples *i.e.* control, T1 and T2. C-H bending (out of plane) peak was found at 931  $\text{cm}^{-1}$  in control and 933  $\text{cm}^{-1}$  in both T1 and T2 sample. The peak due to meta substituted arene was appeared at 748  $\text{cm}^{-1}$  in control and T1 and at 750  $\text{cm}^{-1}$  in T2. The FT-IR spectra were well supported by reference data [31].

The FT-IR spectroscopic study showed that no alteration was found in FT-IR spectra of treated samples (T1 and T2) as compared to

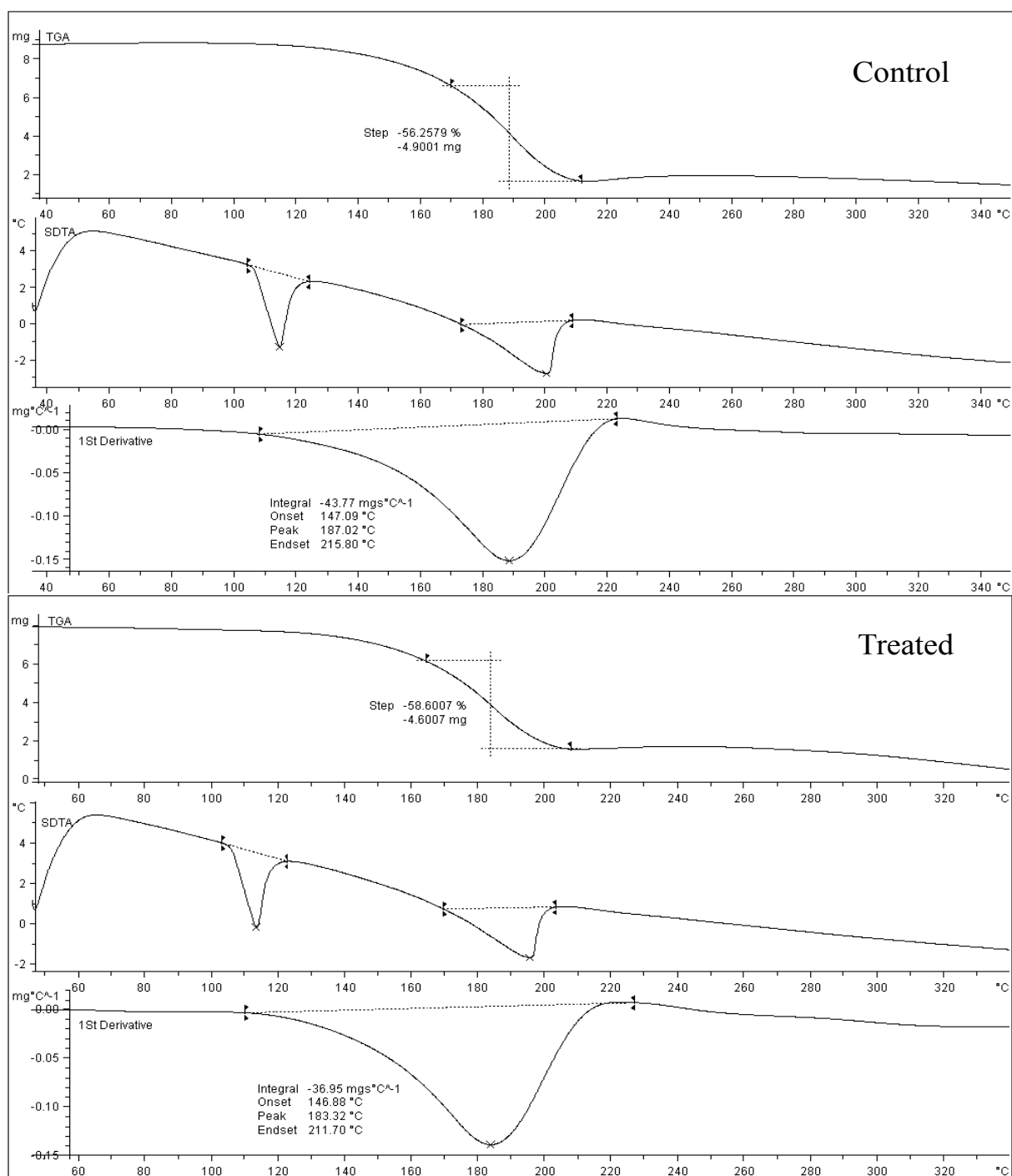


Figure 4: TGA thermogram of control and treated samples of m-toluic acid.

control. It suggests that biofield treatment did not cause any alteration in structural and bonding properties like bond strength, stability, rigidity of structure *etc.*

**UV-Vis spectroscopic analysis:** The UV spectra of control and treated samples (T1 and T2) of MTA are shown in Figure 7. The UV spectrum of control sample showed characteristic absorption at 204 nm which was also observed in both treated samples (T1 and T2) at 203 nm. Another absorption peak was observed at 230 nm in

control sample which was evident in T1 and T2 at 230 nm and 229 nm respectively. The spectrum of control sample showed weak absorption at 278 nm. The treated samples *i.e.* T1 and T2 also showed same kind of peak at 278 nm and 275 nm respectively. The UV spectrum of control MTA was well supported by literature data [32]. It suggests that biofield treatment could not make any alteration in chemical structure or arrangement of functional groups of treated MTA samples.

## Conclusion

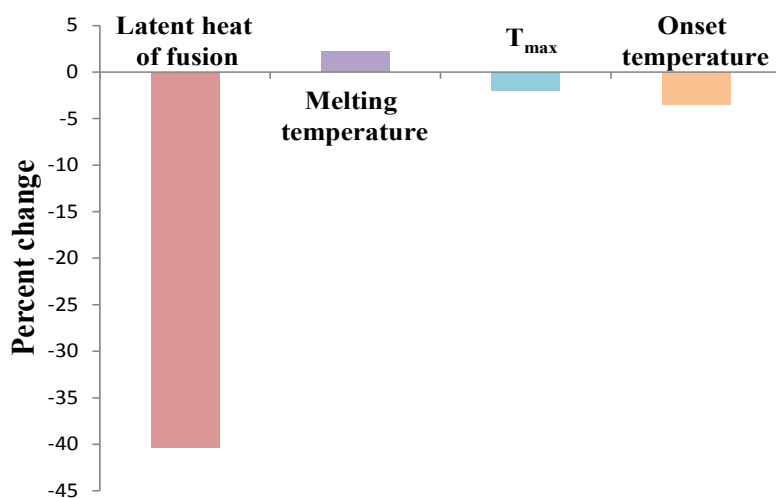


Figure 5: Percent change in latent heat of fusion, melting point, T<sub>max</sub> and onset temperature in biofield treated m-toluic acid with respect to control

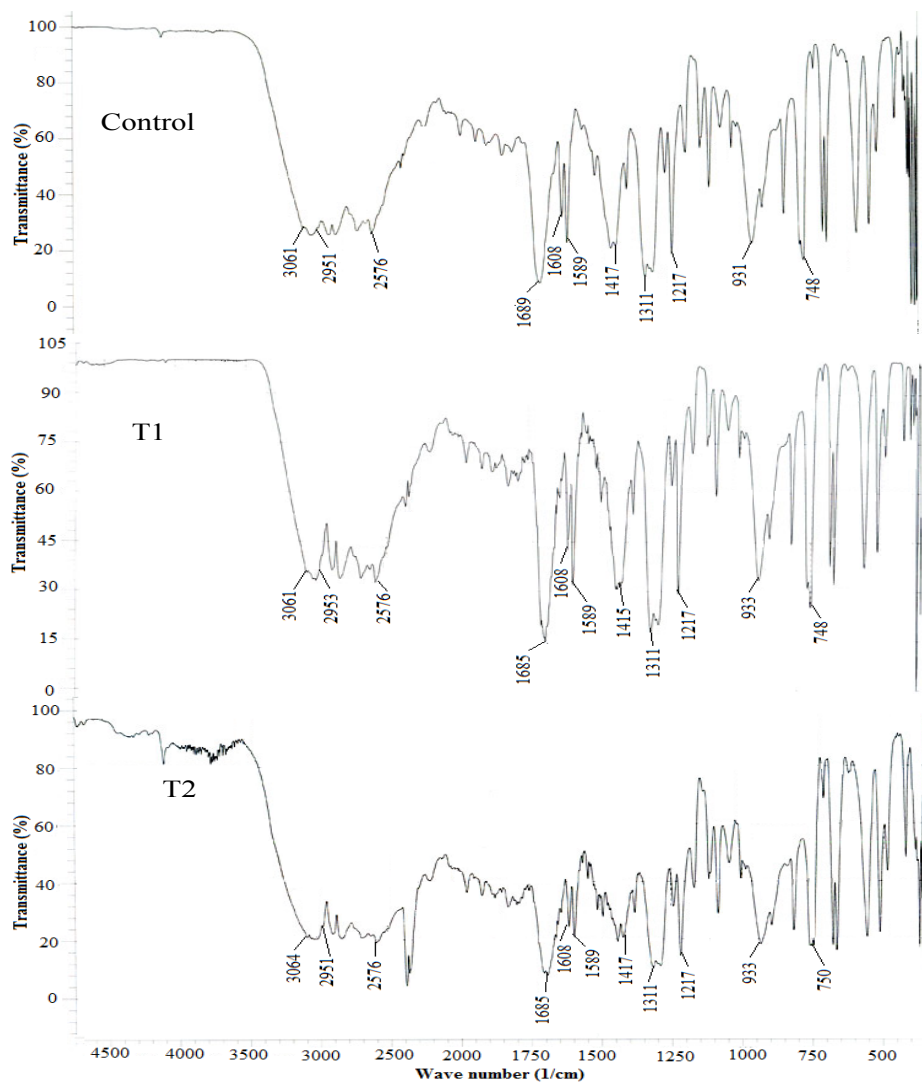


Figure 6: FT-IR spectra of control and treated samples of m-toluic acid.

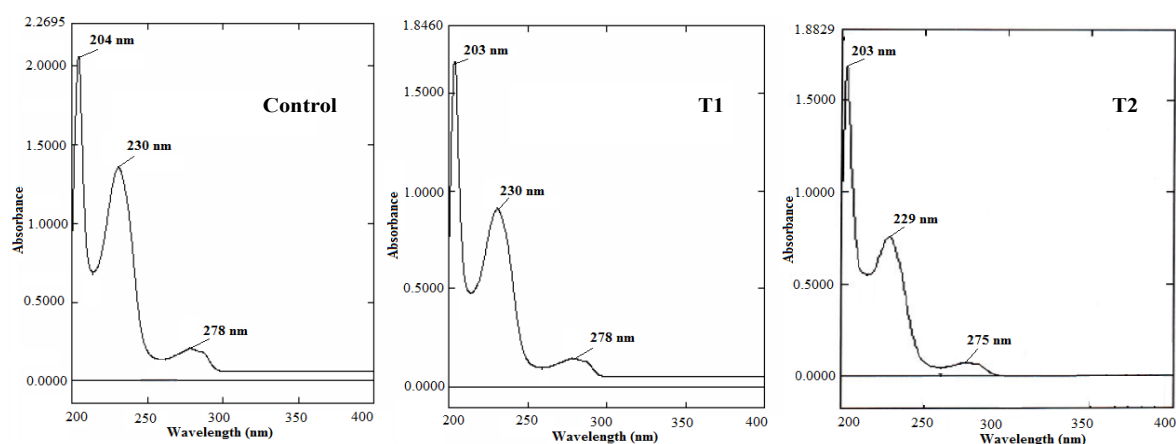


Figure 7: UV-Vis spectra of control and treated samples of m-toluic acid.

The overall study showed the influence of biofield treatment on physical and thermal properties of MTA. XRD result showed that crystallite size was decreased by 42.86% in treated MTA samples as compared to control, which might be due to fracturing of grains into sub grains caused by lattice strain produced *via* biofield energy. The surface area analysis showed an increase in surface area of 107.14% in treated MTA sample as compared to control. The reduced crystallite size and increased surface area may lead to increasing the reaction kinetics of MTA, which could make it more useful as an intermediate compound. Thermal analysis data revealed that latent heat of fusion was reduced by 40.32% in treated MTA as compared to control. TGA/DTG studies showed that  $T_{max}$  was decreased by 1.97% in treated MTA samples. On the basis of reduction in  $T_{max}$ , it is hypothesized that MTA molecules turn into vapour phase at low temperature as compared to control. Hence, molecules in vapour phase may collide more frequently with other reactants in any reaction that might enhance the rate of reaction. Therefore, it is assumed that biofield treated MTA could be more useful as an intermediate in the production of various pharmaceutical products.

#### Acknowledgement

The authors would like to acknowledge the whole team of Sophisticated Analytical Instrument Facility (SAIF), Nagpur, Indian Rubber Manufacturers Research Association (IRMRA), Thane and MG V Pharmacy College, Nashik for providing the instrumental facility. Authors are very grateful for the support of Trivedi Science, Trivedi Master Wellness and Trivedi Testimonials in this research work.

#### Conflict of Interest

The authors declare that they have no competing interest.

#### References

1. Wilson CO (2004) Wilson and Gisvold's textbook of organic medicinal and pharmaceutical. (11th edn), Lippincott Williams & Wilkins, Philadelphia, U.S.
2. [http://www.medipharmlimited.com/whitfield\\_ointment.asp](http://www.medipharmlimited.com/whitfield_ointment.asp)
3. Lillard B (1919) Practical druggist and pharmaceutical review of reviews. Lillard & Company, Michigan, U.S.
4. Knoess PH, Neeland EG (1998) A modified synthesis of the insect repellent DEET. *J Chem Educ* 75: 1267.
5. Bays D, Foster R (1974) Benzoylphenylacetic acids and related compounds. U.S. Patent 3828093.
6. Pavia DL, Lampman GM, Kriz GS, Engel RG (2005) Introduction to organic laboratory techniques: A small scale approach. Cengage Learning, U.S.
7. Carballo LM, Wolf EE (1978) Crystallite size effects during the catalytic oxidation of propylene on Pt/?-Al<sub>2</sub>O<sub>3</sub>. *J Catal* 53: 366-373.
8. Chaudhary AL, Sheppard DA, Paskevicius M, Pistidda C, Dornheim M, et al (2015) Reaction kinetic behaviour with relation to crystallite/grain size dependency in the Mg-Si-H system. *Acta Mater* 95: 244-253.
9. Movaffaghi Z, Farsi M (2009) Biofield therapies: biophysical basis and biological regulations? *Complement Ther Clin Pract* 15: 35-37.
10. Giasson M, Bouchard L (1998) Effect of therapeutic touch on the well-being of persons with terminal cancer. *J Holist Nurs* 16: 383-398.
11. Peck SD (1998) The efficacy of therapeutic touch for improving functional ability in elders with degenerative arthritis. *Nurs Sci Q* 11: 123-132.
12. Turner JG, Clark AJ, Gauthier DK, Williams M (1998) The effect of therapeutic touch on pain and anxiety in burn patients. *J Adv Nurs* 28: 10-20.
13. Mager J, Moore D, Bendl D, Wong B, Rachlin K, et al. (2007) Evaluating biofield treatments in a cell culture model of oxidative stress. *Explore (NY)* 3: 386-390.
14. Trivedi MK, Bhardwaj Y, Patil S, Shettigar H, Bulbule A (2009) Impact of an external energy on *Enterococcus faecalis* [ATCC-51299] in relation to antibiotic susceptibility and biochemical reactions-an experimental study. *J Accord Integr Med* 5: 119-130.
15. Trivedi MK, Patil S (2008) Impact of an external energy on *Staphylococcus epidermidis* [ATCC-13518] in relation to antibiotic susceptibility and biochemical reactions-an experimental study. *J Accord Integr Med* 4: 230-235.
16. Trivedi MK, Patil S (2008) Impact of an external energy on *Yersinia enterocolitica* [ATCC-23715] in relation to antibiotic susceptibility and biochemical reactions: An experimental study. *Internet J Alternat Med* 6: 13.
17. Shinde V, Sances F, Patil S, Spence A (2012) Impact of biofield treatment on growth and yield of lettuce and tomato. *Aust J Basic Appl Sci* 6: 100-105.
18. Sances F, Flora E, Patil S, Spence A, Shinde V (2013) Impact of biofield treatment on ginseng and organic blueberry yield. *Agrivita J Agric Sci* 35: 22-29.
19. Patil SA, Nayak GB, Barve SS, Tembe RP, Khan RR (2012) Impact of biofield treatment on growth and anatomical characteristics of *Pogostemon cablin* (Benth.). *Biotechnology* 11: 154-162.
20. Altekar N, Nayak G (2015) Effect of biofield treatment on plant growth and adaptation. *J Environ Health Sci* 1: 1-9.
21. Dabhade VV, Tallapragada RR, Trivedi MK (2009) Effect of external energy on atomic, crystalline and powder characteristics of antimony and bismuth powders. *Bull Mater Sci* 32: 471-479.
22. Trivedi MK, Nayak G, Patil S, Tallapragada RM, Latiyal O, et al. (2015) Studies of the atomic and crystalline characteristics of ceramic oxide nano powders after bio field treatment. *Ind Eng Manage* 4: 161.
23. Trivedi MK, Tallapragada RR (2008) A transcendental to changing metal powder characteristics. *Met Powder Rep* 63: 22-28.

24. Pavia DL, Lampman GM, Kriz GS (2001) Introduction to spectroscopy. (3rd edn), Thomson Learning, Singapore.
25. Okada K, Nagashima T, Kameshima Y, Yasumori A, Tsukada T (2002) Relationship between formation conditions, properties, and crystallite size of boehmite. *J Colloid Interface Sci* 253: 308-314.
26. Espenson JH (1995) Chemical kinetics and reaction mechanisms. (2nd edn) McGraw-Hill, U.S.
27. Moore J (2010) Chemistry: The molecular science. (4th edn), Brooks Cole, Belmont, U.S.
28. Trivedi MK, Patil S, Tallapragada RM (2013) Effect of biofield treatment on the physical and thermal characteristics of silicon, tin and lead powders. *J Material Sci Eng* 2: 125.
29. Morrell CE, Beach LK (1948) Oxidation of aromatic compounds. U.S. Patent 2443832.
30. Hull EH (1979) Production of N,N-di(ethyl)-meta-toluamide from meta-toluic acid by liquid phase catalytic reaction with diethylamine. U.S. Patent 4133833.
31. Cutler HG (1999) Biologically active natural products: Agrochemicals. CRC Press, U.S.
32. Lang L (1969) Absorption spectra in the ultraviolet and visible region. *Akademiai Kiado Publishers Budapest* 10: 115-400.